AD 424733L

HOWARD UNIVERSITY

DEPARTMENT OF CHEMISTRY

WASHINGTON, D. C.

FINAL REPORT

27 March 1961 to 26 March 1963

MICROWAVE SPECTRA AND DIELECTRIC PROPERTIES OF VARIOUS AZIDES

Contract DA-44-009-ENG-4763
Project No. 8F07-11-001-02

U. S. Army Engineer Research and Development Laboratories

Fort Belvoir, Virginia

Submitted by:

George C. Turrell
Department of Chemistry
Howard University
Washington 1, D.C.

Abstract

Design details are presented for an instrument for the measurement of the dielectric constant and loss tangent of small crystals at millimeter wavelengths. A reflection technique is used to determine changes in the resonant frequency and Q of a TM_{012}-mode cavity. The instrument, which is now completed, will be used in dielectric studies on α- and β-lead azide crystals in the region from 40 to 50 KMcs and upwards.

A Stark-modulated microwave spectrograph is described, along with a phase-stabilized klystron source which is to be added to the system. The basic instrument is currently being tested.

The Appendix contains a discussion of the infrared spectrum of solid methyl azide, which has been observed over the range 400 to 40[illegible] cm^{-1}. Some changes in vibrational assignments for the molecule are suggested. No evidence of hydrogen bonding has been found in the solid.

CONTENTS

I. DIELECTRIC MEASUREMENTS AT MILLIMETER WAVELENGTHS

In an isotropic material in which the electromagnetic field equations are linear, the dielectric properties are specified by the complex dielectric constant

$$\epsilon = \epsilon' - j\epsilon'' = \epsilon' [1 - \tan\delta]. \quad [1]$$

The dimensionless quantity $\tan\delta$, called the loss tangent, is equal to the power dissipated divided by the power stored per cycle and is thus a measure of the energy lost in the form of heat when an electromagnetic wave is propagated through the material.

Principle of the Method

The usual methods of measuring ϵ' and ϵ'' at microwave frequencies involve either loading a waveguide with a slab of the dielectric material[1] or mounting a thin rod of the material in a resonant cavity parallel to the electric field, the length of the rod being equal to the height of the cavity.[2] Either of these methods involves obtaining an accurate fit of the sample in the microwave circuit. This requirement places serious limitations on the shape and size of samples. Furthermore, with hard, brittle materials attaining an exact fit is a difficult problem because the edges of the sample tend to chip and crack. Another disadvantage is that the waveguide or cavity must be disassembled for correct positioning of the sample. Hence it becomes difficult to reproduce the electrical characteristics of the cavity or waveguide in the empty state.

In the present work the technique developed by Labuda and

I. DIELECTRIC MEASUREMENTS AT MILLIMETER WAVELENGTHS

In an isotropic material in which the electromagnetic field equations are linear, the dielectric properties are specified by the complex dielectric constant

$$\epsilon = \epsilon' - j\epsilon'' = \epsilon' [1 - \tan\delta]. \quad [1]$$

The dimensionless quantity $\tan\delta$, called the loss tangent, is equal to the power dissipated divided by the power stored per cycle and is thus a measure of the energy lost in the form of heat when an electromagnetic wave is propagated through the material.

Principle of the Method

The usual methods of measuring ϵ' and ϵ'' at microwave frequencies involve either loading a waveguide with a slab of the dielectric material[1] or mounting a thin rod of the material in a resonant cavity parallel to the electric field, the length of the rod being equal to the height of the cavity.[2] Either of these methods involves obtaining an accurate fit of the sample in the microwave circuit. This requirement places serious limitations on the shape and size of samples. Furthermore, with hard, brittle materials attaining an exact fit is a difficult problem because the edges of the sample tend to chip and crack. Another disadvantage is that the waveguide or cavity must be disassembled for correct positioning of the sample. Hence it becomes difficult to reproduce the electrical characteristics of the cavity or waveguide in the empty state.

In the present work the technique developed by Labuda and

LeCraw[3] has been adopted. This method employs a TM_{012}-mode cylindrical cavity with the sample in the form of a thin rod suspended away from all walls. In the TM_{012} mode the electric field exhibits a maximum in the center of the cavity and minima at approximately 1/4 and 3/4 the cavity height. Thus by using samples in the form of rods or needles which have been trimmed to about one-half the cavity height and positioning them so that their ends fall at the nodes, the measurement becomes quite insensitive to the exact shape and size of the sample.

As in the usual cavity method, a perturbation calculation is used to relate the shift in resonant frequency and the change in loaded Q of the cavity to the complex dielectric constant of the sample causing the change. The basic assumption of perturbation theory for this application is that changes in the configuration of the rf fields must be small upon introduction of the sample.

The perturbation equation for the case of a thin rod in a TM_{012}-mod cavity as described above has been derived by Labuda and LeCraw[3] in the form

$$\frac{f - f_o}{f_o} + j \frac{1}{2}\left(\frac{1}{Q_L} - \frac{1}{Q_L^o}\right) = -\left(\frac{\epsilon}{\epsilon_o} - 1\right) G \frac{V_s}{V_c} . \quad [2]$$

The constant G is a dimensionless geometrical factor and is given by

$$G = 0.0680/\mu_o \epsilon_o f_o^2 D^2 , \quad [3]$$

where D is the diameter of the cavity. Separation of the real and imaginary parts of Eq. [2] yields the relations

$$\frac{f - f_o}{f_o} = -\left(\frac{\epsilon'}{\epsilon_o} - 1\right) G \frac{V_s}{V_c} \quad [4]$$

and

$$(1/2)\left(\frac{1}{Q_L} - \frac{1}{Q_L^o}\right) = \frac{\epsilon''}{\epsilon_o} \; G \; \frac{V_s}{V_c} \quad , \qquad [5]$$

where Q_L^o is the loaded Q of the empty cavity and Q_L is the loaded Q of the cavity containing the sample. The volumes of the cavity and the sample are represented by V_c and V_s, respectively.

The method outlined above provides a convenient technique for determining ϵ' and ϵ'' in terms of the cavity dimensions and the sample volume, provided that direct and accurate measurements of the frequency shifts and the appropriate loaded Q's can be made.

Cavity Design

The resonant frequencies of a right-circular, cylindrical cavity are divided into TE- [transverse electric] and TM- [transverse magnetic] classes, where the axis of reference is along the cylinder axis. They are further specified in terms of three integers ℓ, m and n which are defined by

ℓ ≡ number of full-period variations of E_r with respect to θ,

m ≡ number of half-period variations of E_θ with respect to r, and

n ≡ number of half-period variations of E_r with respect to z,

for the TE modes. For TM modes the integers are correspondingly defined in terms of the components of the magnetic field.

The resonant frequencies are given by[4]

$$[fD]^2 = [cx_{\ell m}/\pi]^2 + [cn/2]^2[D/L]^2 \quad , \qquad [6]$$

where L is the height of the cavity and, for TM modes, $x_{\ell m} \equiv m^{th}$ root of the Bossel function $J_\ell[x] = 0$.

The first cavity was designed for a resonant frequency of 40 KMcs. This frequency represents the lower end of the range of interest and hence

involves the largest samples needed. Furthermore, klystrons and waveguide components were already on hand for work at this frequency.

The Q of the cavity is quite insensitive to the ratio D/L, hence the value D = 0.300" was chosen rather arbitrarily. With $x_{01} = 2.45$ one finds from Eq. [6] that L = 0.448". The cavity was iris-coupled to the waveguide through a 0.073"-diameter hole. The complete design is shown in Fig. 1.

Samples are cemented to nylon threads at each end. The lower thread passes out through a small hole in the bottom of the cavity and is tied to a five gram weight. The upper thread passes through a hole in the top of the cavity and is connected to a micrometer head which is mounted directly above it. Thus samples up to 0.038" in diameter can be introduced into the cavity without disassembling it. The samples can be accurately positioned along the vertical by adjusting the micrometer head.

In the work being carried out under the present Contract, measurements are to be made at least every kilomegacycle over the range 40 to 120 KMcs. It was therfore essential to develop a convenient, easily tunable cavity of sufficiently high Q to facilitate the dielectric measurements. The cavity shown in Fig. 2. has been constructed for this application. Several features of its design are worthy of comment.

Tuning is accomplished by means of a $3\lambda/4$-choke plunger driven by a micrometer. The plunger slides on a teflon bearing to maintain centering and perpendicularity. A long hole through the micrometer shaft, which terminates in a 0.013"-diameter hole in the center of the

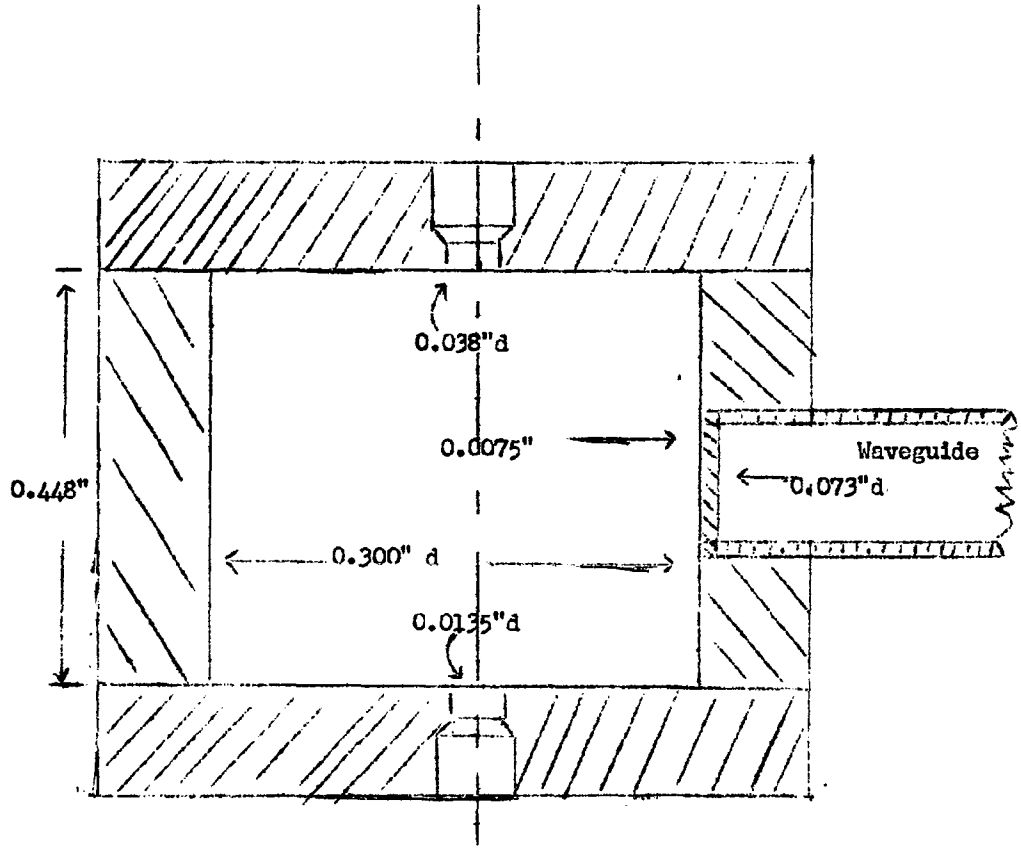

Fig. 1. Microwave Cavity

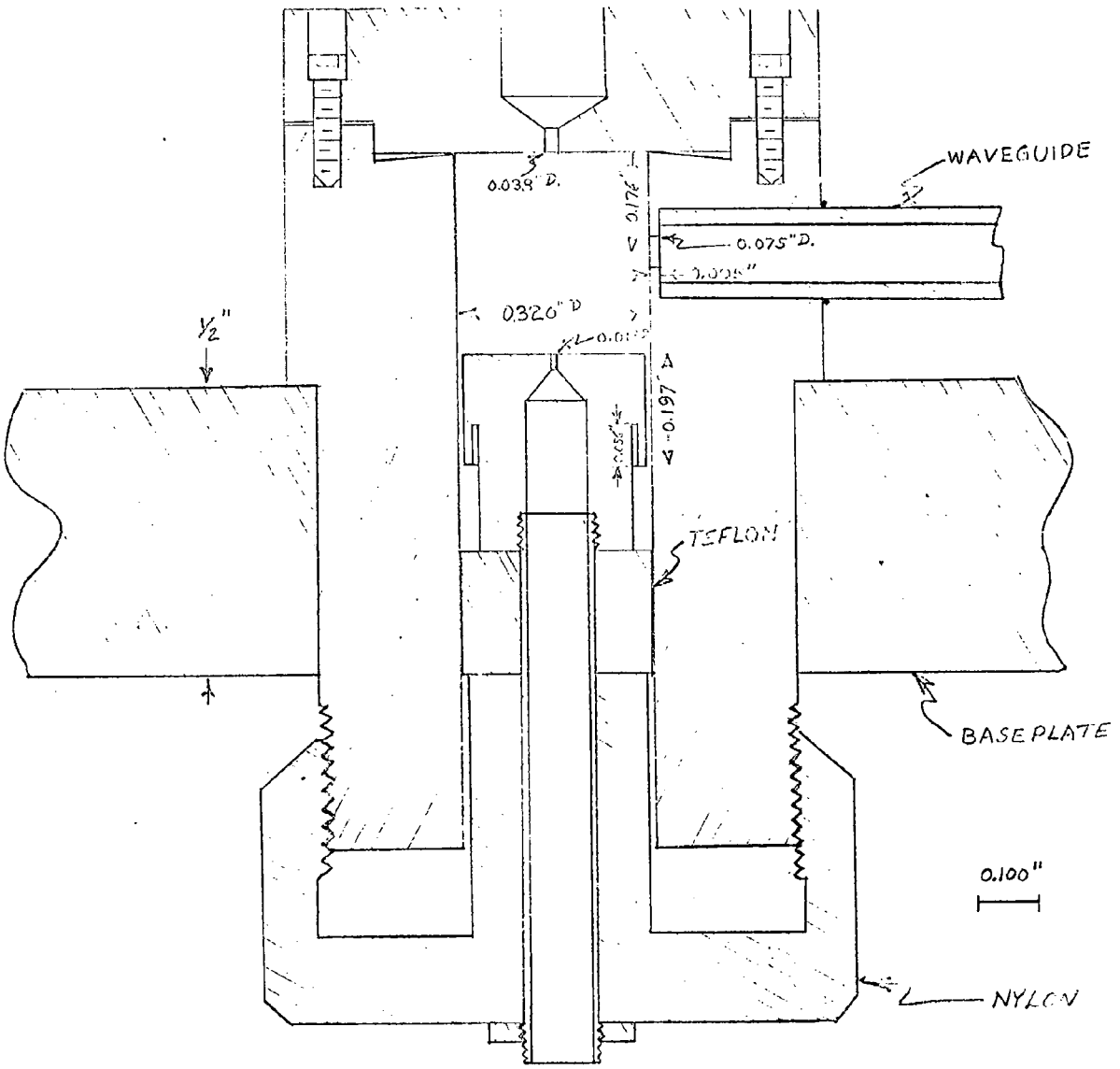

Fig. 2. Resonant Cavity (45 KMcs.)

plunger, allows a nylon thread to pass through the bottom of the cell. The thread is cemented to the crystal and tied to a small weight to insure proper allignment of the sample. The crystal is supported by another thread, which is connected to the micrometer head mounted above the cavity as described above.

The electrical design of the tuning plunger is optimum at a frequency of 40 KMcs. and provides a useful tuning range of 40 to 50 KMcs. The cavity diameter was chosen so that the travel of the plunger could be kept small for the 10 KMcs. range, while not introducing too large a setting error in the resonant frequency. The iris coupling hole is centered vertically at a frequency of 45 KMcs. No effort was made to adjust the iris diameter to achieve critical coupling, as one can critically couple the cavity at any designed frequency by simple adjustments of the E-H tuner in the external circuit.

Measurement of Q_L

A sweep-frequency method of measuring the Q of single-ended resonators by observing the variation of reflected power with frequency has been described by E. D. Reed.[5] In the present work Reed's method has been adapted to the experimental determination of frequency shifts and changes in loaded Q upon introduction of a dielectric sample. The waveguide circuit used in these experiments is shown in Fig. 3.

Power from the klystron source [Polarad type S3742-1 EHF Source powered by a type HU-1] is split by the magic tee, half of it passing through a calibrated attenuator to a tunable crystal detector which monitors the output of the klystron. Power from the other E-plane

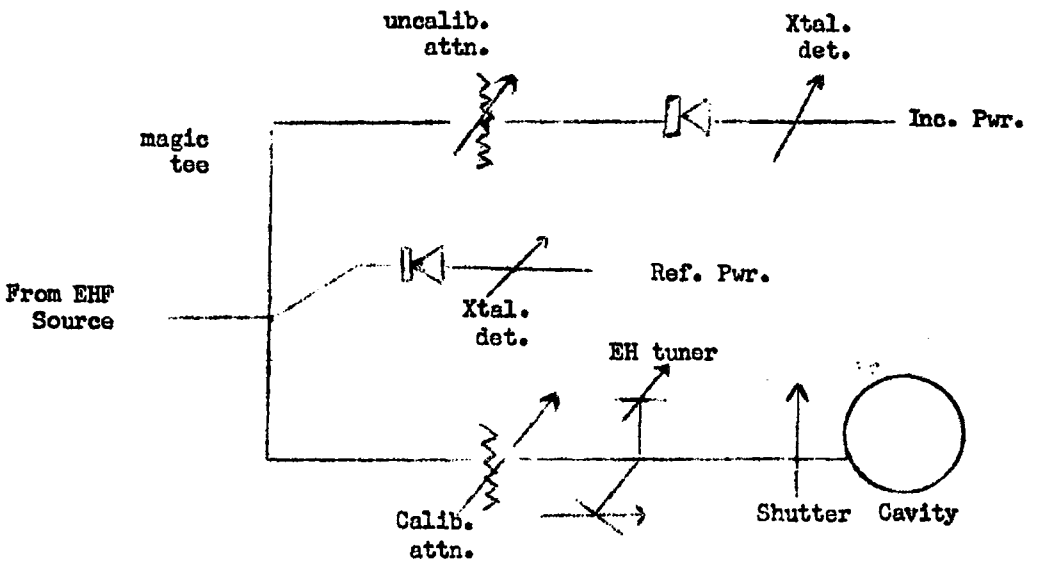

Fig. 3. Waveguide Circuit

branch of the magic tee passes through an uncalibrated attenuator and is critically coupled to the cavity by means of an E-H tuner. Power reflected from the cavity is detected by a tunable crystal detector connected to the H-plane branch of the magic tee.

The waveguide shutter indicated in Fig. 3. was not available commercially. It was therefore developed especially for this application as shown in Fig. 4. A phosphor-bronze sliding shutter slides in a brass housing. Effective electrical contact is provided by circular chokes at either side of the shutter. The dimensions of the chokes were calculated by sealing the dimensions of commercial choke-flanges. Performance data on this unit have not yet been obtained.

The power reflected from the cavity, as well as that incident upon it, are displayed on the oscilloscope [Tektronix type 515A] using the circuit diagrammed in Fig. 5. Two of the channels of the four-channel amplifier [Tektronix type M powered by a type 132] are used to amplify the detected incident and reflected power. The input to a third channel is short-circuited to provide a reference zero-power level. Modulation for the klystron is provided by the sweep output of the oscilloscope. The gate output of the oscilloscope produces the switching trigger for the four-channel amplifier.

Frequency markers are inserted on the display by means of the following scheme. A sample of the klystron power is split off at the output of the source unit using another magic tee with a terminated H-plane branch. The sample power is sent to a spectrum analyzer [Polarad type TSA equipped with a type STU-5 tuning unit] which has been modified as follows. The saw-tooth voltage which drives the sweeping local oscillator was disconnected. The marker oscillator was disconnected and replaced by a General Radio type 1330-A rf

SHUTTER AND CHOKE FLANGES

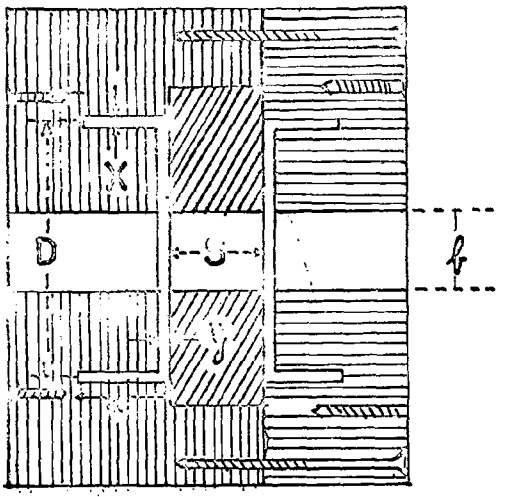

D = 0.306
d = 0.081
X = 0.020
y = 0.002
S = 0.081
f = 0.112
a = 0.224

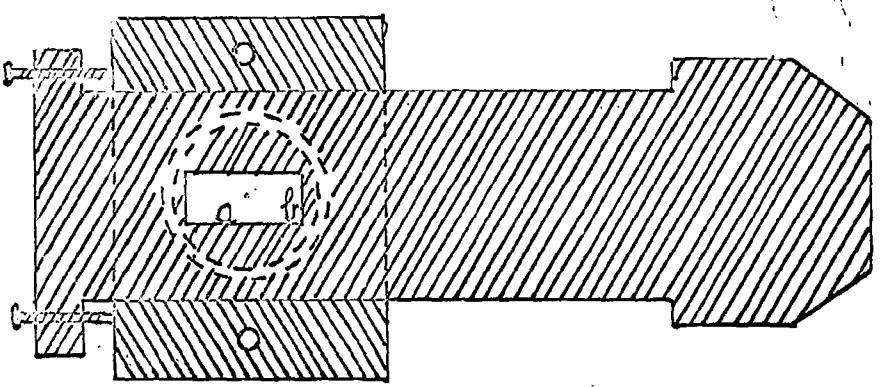

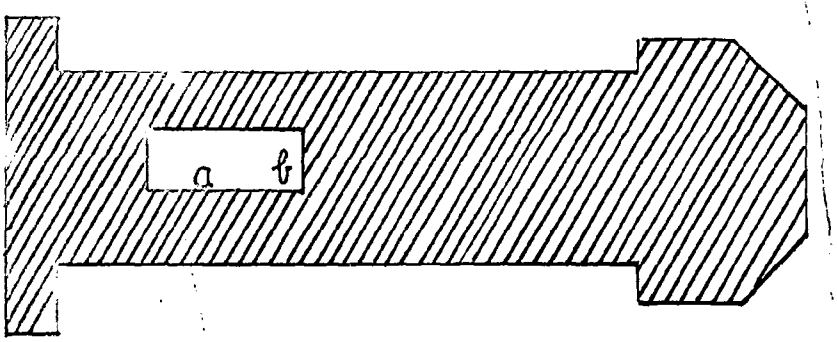

Fig. 4.

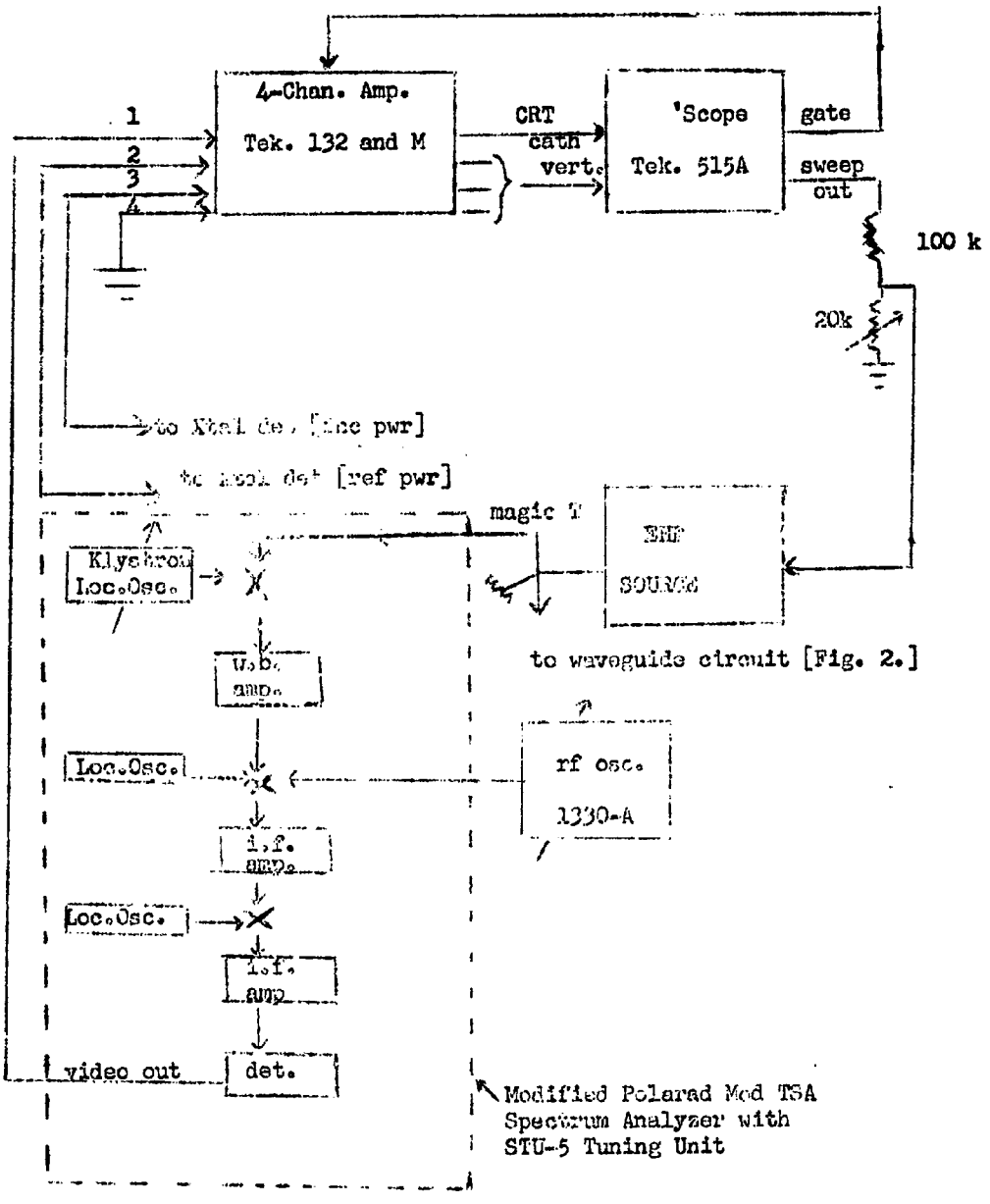

Fig. 5. Block Diagram of Control and Display Circuitry

oscillator. The video output of the analyzer was amplified by the fourth channel of the type M before being connected to the cathode of the type 515A's cathode-ray tube. Hence the trace on the oscilloscope receives a blanking pulse each time the input frequency, the klystron local oscillator frequency and 224 Mcs. from the local oscillator mix to produce a signal at the first IF amplifier at a frequency of 64 Mcs. In addition a pulse [and hence a corresponding blank spot on the oscilloscope screen] will appear at each side of the central pulse and separated from it by the frequency of the General Radio oscillator. A typical oscilloscopic display is sketched in Fig. 6.

In actual operation the system is balanced with the shutter in the short-circuit position and the calibrated attenuator set at about 20 db. The uncalibrated attenuator is adjusted until the incident and reflected traces match. The shutter is then opened to connect the cavity to the circuit, and the calibrated attenuator is advanced to a new value, say 23 db. The central marker is then set on the reflected power minimum by adjusting the klystron local oscillator frequency and the General Radio oscillator is adjusted until the side markers are coincident with the intersections of the incident-and reflected-power traces.

If the calibrated attenuator was advanced by expactly 3 db., then the loaded Q is given by

$$Q_L^o = f_o/\Delta f \quad , \qquad [7]$$

where Δf is twice the reading on the General Radio oscillator and f_o can be measured directly by inserting the wave-meter marker on the EHF source unit.

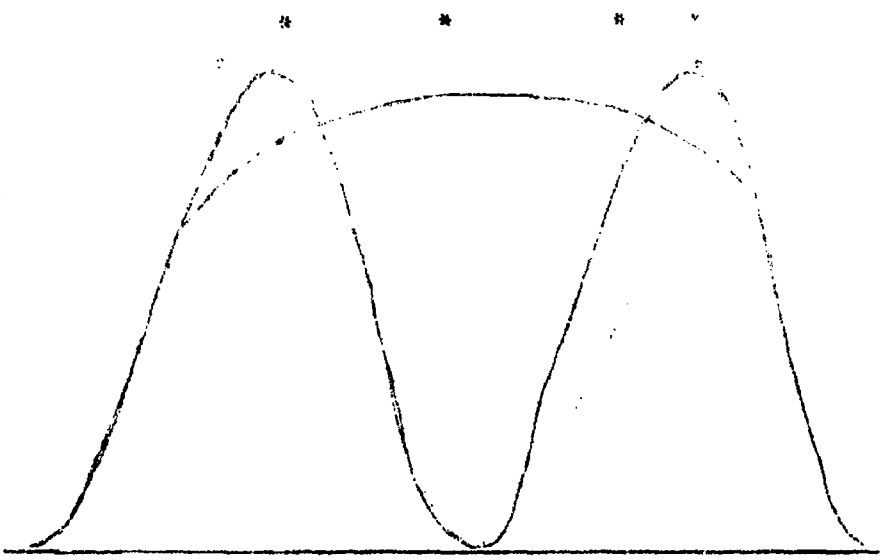

Fig. 6. Oscilloscope Display.

The incident power has been attenuated. Note frequency markers [trace blanked] below asterisks.

The same procedure carried out with the sample in place yields a value for Q_L. The frequency shift caused by introduction of the sample can be measured directly by leaving the central marker on the reflected-power minimum when the cavity is empty, inserting the sample, and tuning the General Radio oscillator until one of the side markers coincides with the reflected-power minimum from the cavity containing the sample. The reading on the oscillator is then equal to $f-f_0$. This procedure provides a direct and accurate measurement of $f-f_0$ which cannot possibly be obtained as the difference between two wave-meter readings.

Initial tests of the above scheme have been made using thin rods of polystyrene. A resonance in the first cavity which was found at 39,830 Mcs. was proven to be the TM_{012} mode by observing the resonant frequency as a function of insertion of a short polystyrene rod as measured on the micrometer head. A frequency minimum [maximum shift] was observed when the rod was centered along the axis of the cavity, while frequency maxima [nearly as high as the resonant frequency of the empty cavity] were observed when the rod was centered on L/4 and 3L/4.

As designed, the cavity was found to be somewhat undercoupled [$Q_0 < Q_E$, where Q_0 is the internal Q of the cavity and Q_E is the Q of the external circuit]. This situation is easily corrected by adjustment of the E-H tuner [see Fig. 3.] to bring the reflected-power trace at the resonant frequency down to the zero-power level, as shown in Fig. 6. Under this condition [critical coupling] $Q_0 = Q_E$, hence

$$\frac{1}{Q_L} = \frac{1}{Q_0} + \frac{1}{Q_E} = \frac{2}{Q_0} \qquad [8]$$

and $Q_0 = 2\,Q_L$.

A rough measurement of the internal Q of the first cavity yielded a value in the neighborhood of 1000. The theoretical internal Q of a cavity of this geometry is nearly 3500. Hence, it would seem that the cavity walls are not as well-machined as they should be. Re-machining, as well as silver plating, might be resorted to in an effort to bring up the value of Q_0. In the method outlined above it is distinctly advantageous to employ a cavity whose Q_0 is high enough so that the entire resonance curve is somewhat narrower than the source klystron's mode pattern. In this case the Q measurement can be made without the necessity of retuning the klystron.

Determination of Sample Volume

Equations [4] and [5] indicate that the determination of either component of the complex dielectric constant depends upon a knowledge of the volume of the sample used. For the small crystalline samples of alpha lead azide which are now being tried, the volume determination is quite difficult. This problem would be eliminated if reliable density data were available on this material. As no such data have been found in the literature, it will be necessary in the present work to assume that the theoretical densities calculated from the crystallographic data[6] are valid. For the alpha and beta forms of lead azide, values of 4.76 and 4.91 g/cm^3, respectively, were obtained. These data will be combined with micro-weighings of the samples to yield the necessary volumes. A Cahn microelectrobalance has been purchased to facilitate the weighings.

STATUS OF WORK

Work on the dielectric measurements has been interrupted for several

months due to electronic failures. A severe frequency jitter developed on the marker [blanking] signal. Such instability could arise from variations in either the source klystron [or its power supplies] or in the spectrum analyzer. The latter unit was found to perform somewhat below specifications, although it was not primarily responsible for the observed frequency jitter. Attention was therefore focussed on the EHF source. The QK293 klystron was replaced and all power supplies were checked for ripple. However, the source of the jitter was not determined. The units were then turned over to the instrument shop at ERDL. After several weeks the trouble was not located and, furthermore, the QK293 was no longer operative. Both units have now been returned to the Polarad Corporation in New York for overhaul. In the meantime a new General Radio Oscillator [Model 1211-C] was purchased to replace the Model 1330-A, thus providing higher accuracy in the frequency-shift measurements.

II. MICROWAVE SPECTROGRAPH

The design details of a Stark-modulated, frequency-stabilized microwave spectrograph have now been completed. The instrument, with the appropriate sources, will, in principle, be capable of investigating spectra throughout the microwave region. [Currently, supplies are on hand only for the region from 20 Gcs/sec to 37.5 Gc/sec.] By using a phase-stabilized kystron source, it will be possible to employ sweep rates as low as a few hundred kilocycles per hour. The use of such slow sweeps results in very high-resolution spectra and greater accuracy in measuring line frequencies. Furthermore, a high resolution instrument yields more information concerning quadrupole interactions, line shapes, and other details of molecular spectra in the microwave region.

GENERAL DESCRIPTION

The general block diagram of the instrument appears in Fig. 1. A diagram and a detailed explanation of the individual blocks appears later. Block 1 constitutes a frequency multiplier whose output is derived from WWV, the radio station of the National Bureau of Standards. This frequency is used to phase-lock a reference klystron operating at approximately 3000 Mc/sec. [Block 2]. Stabilization is achieved by mixing the klystron output with harmonics of the standard frequency and phase detecting the resulting beat frequency. The DC output of the phase detector is then connected in series with the klystron reflector supply to correct for any frequency deviation. Thus, the ouput is a clean frequency standard at 3000 Mc/sec, with the stability of WWV [or governing crystal].

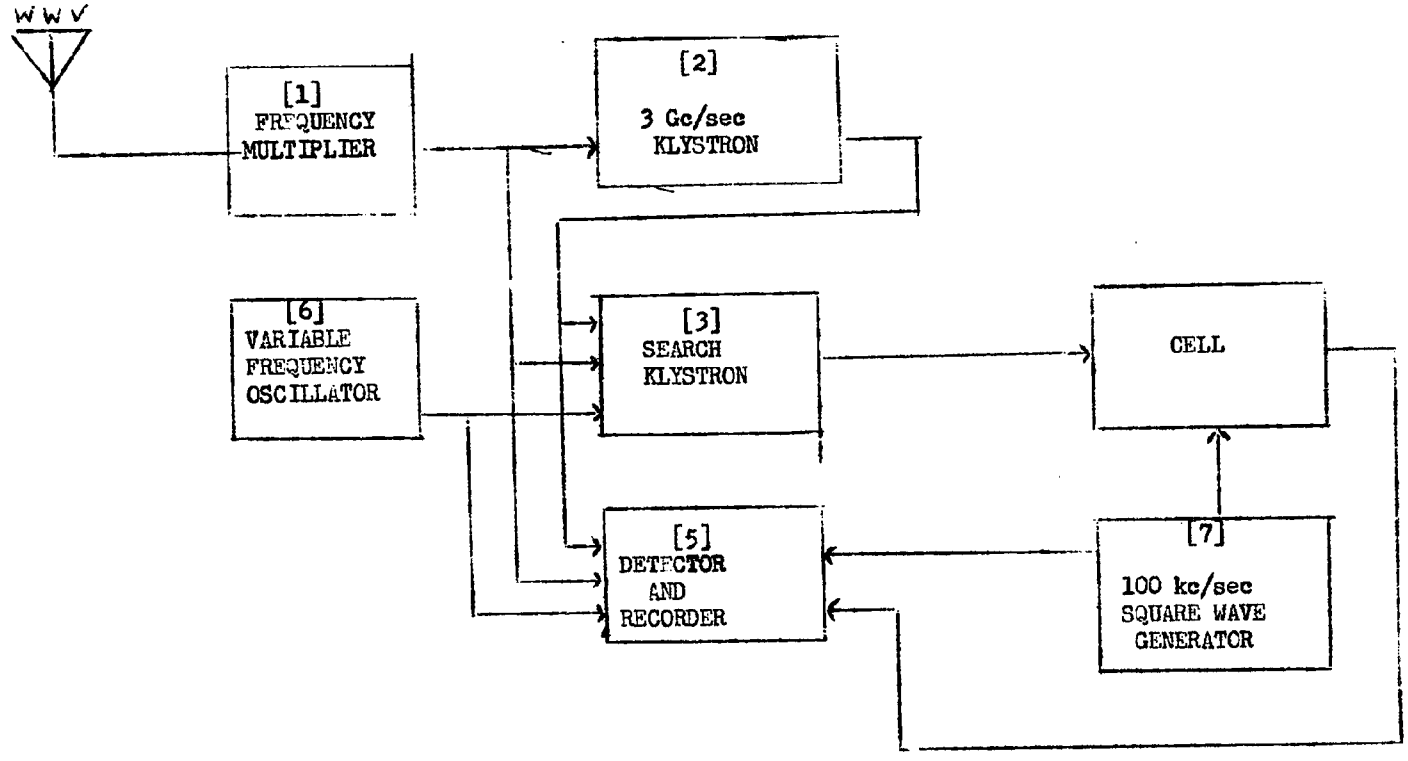

Fig. 1. Block Diagram of Spectrometer

The search klystron [Block 3] is now phase-locked with the reference klystron and the output of a variable-frequency oscillator [VFO]. Locking is achieved by mixing the search frequency with the harmonics of the 3000 Mc/sec standard and then mixing the resulting beat [which is somewhere between zero and 3000 Mc/sec] with harmonics of the VFO. The new beat frequency is phase-detected and used to control the search klystron frequency in the same manner as above. The result of this scheme is a variable microwave frequency with a sufficiently narrow instantaneous frequency spectrum so that it can be swept extremely slowly through any convenient region. The frequency stability of the system is determined both by the 3000 Mc/sec standard and the VFO, although the stability of the latter is less important, as will be shown later.

The output of the search klystron passes through the Stark cell [Block 4], where the sample is located. The optional Stark modulation is accomplished by means of a 100 kc/sec square wave applied to the septum in the cell described below. The signal leaving the cell is amplified, detected and recorded. The possibility of a heterodyne detection system is included in the design.

DETAILED DESCRIPTION

Figure 2. shows the details of the frequency standard, Block 1. The basis for the standard is either the 15 Mcs carrier from WWV or a crystal-controlled 1 Mc/sec signal which is the time base for a Hewlett-Packard type 5243L frequency counter. [The latter signal is multiplied to 5 Mc/sec and then to 15 Mc/sec.] The chain is split, and on one side the signal is multiplied to 405 Mc/sec for use in the 3000 Mc.sec standard. On the other side the signal is multiplied to 30 Mc/sec, a frequency with

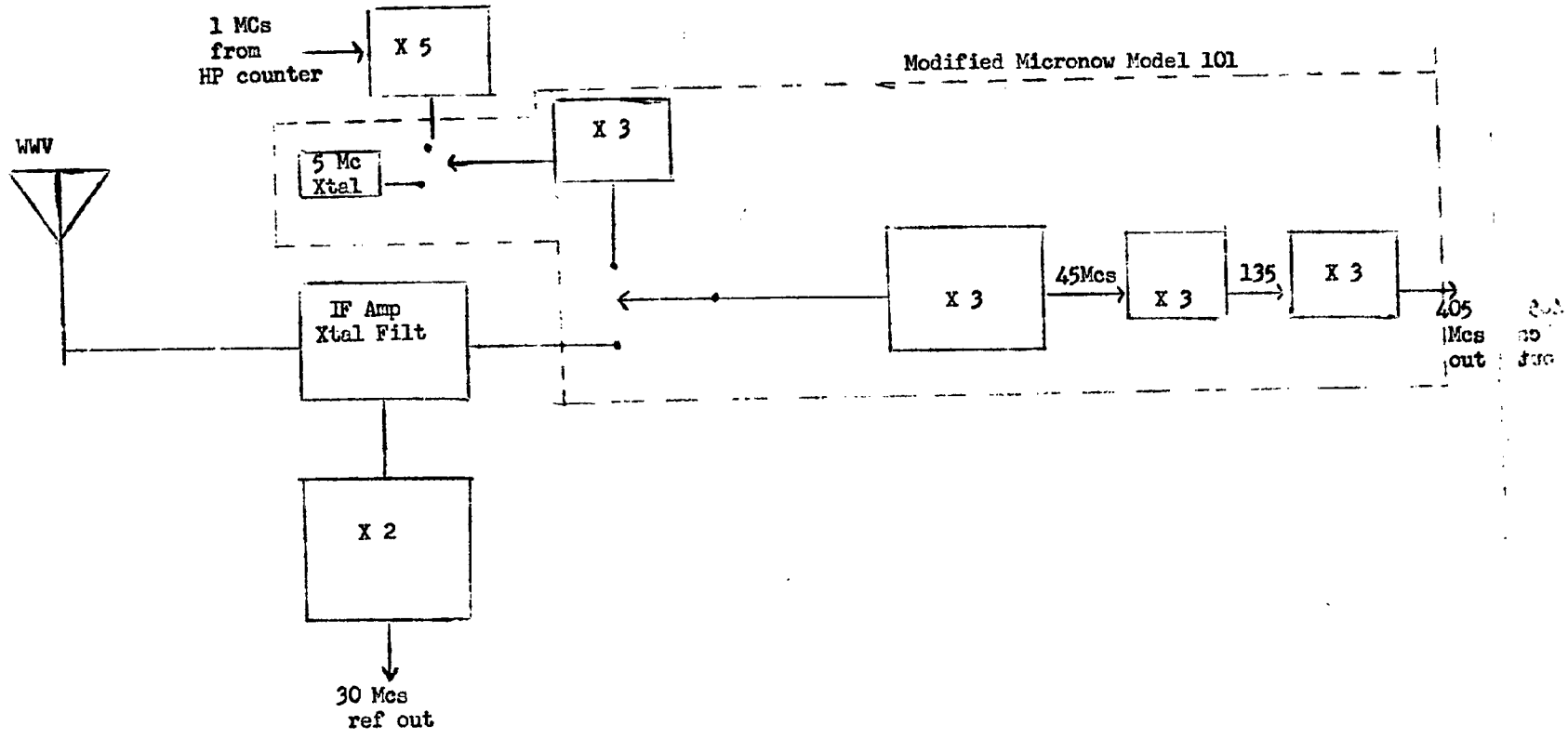

Fig. 2. Low-Frequency Standard

many uses in this system.

The 3000 Mc/sec standard is diagrammed in Fig. 3. The klystron output is divided four ways by a coaxial power divider. Two of the four outputs are used elsewhere in the system and the third goes to a wavemeter for frequency measurement. The fourth output is mixed with harmonics of the 405 Mc/sec signal. The resultant beat is amplified in a tuned 60 Mc/sec amplifier, and phase-detected. The DC output of the detector is used as an error signal to correct the klystron reflector voltage. That this system will indeed lock in on a certain frequency can be seen by a consideration of the action of a phase detector.

Figure 4. contains the diagram of a sample diode phase detector. The signal voltage E_s is applied to the two diodes in push-pull, but the reference voltage E_r is applied in phase. In practice, $E_r \gg E_s$. If the signal voltage is zero, the reference develops the same voltage at points P and R [with respect to point Q] making the output V equal to zero. The presence of a signal voltage will add to one point and subtract from the other [of points P and R] depending on the phase relationship at the time. Since $E_r \gg E_s$, the only time an output signal is produced is when point B is positive with respect to point Q. The integrating network serves to average the voltages over this entire period. With two signals of exactly the same frequency, the output V will depend on the difference in phase between them. It will be zero when the phase difference is such that during the time that B is positive, the voltages at A and C are [averaged over the half-cycle] identical. This relationship will occur only when the phase difference between the two signals is 90 degrees. Any other phase difference will upset the balance and result in a positive or negative value of V.

Suppose that the two signals are of slightly different frequency.

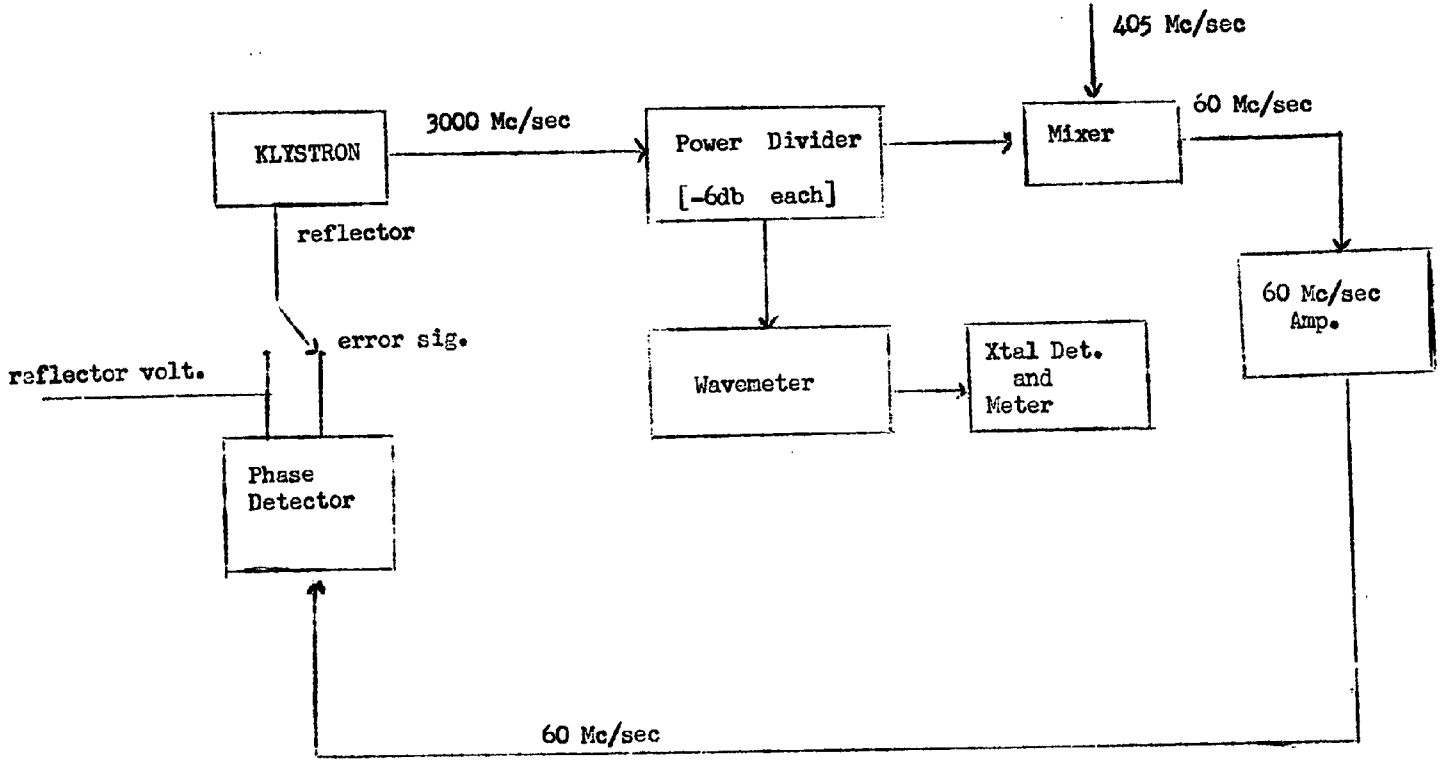

Fig. 3. 3000 Mc/sec. Standard

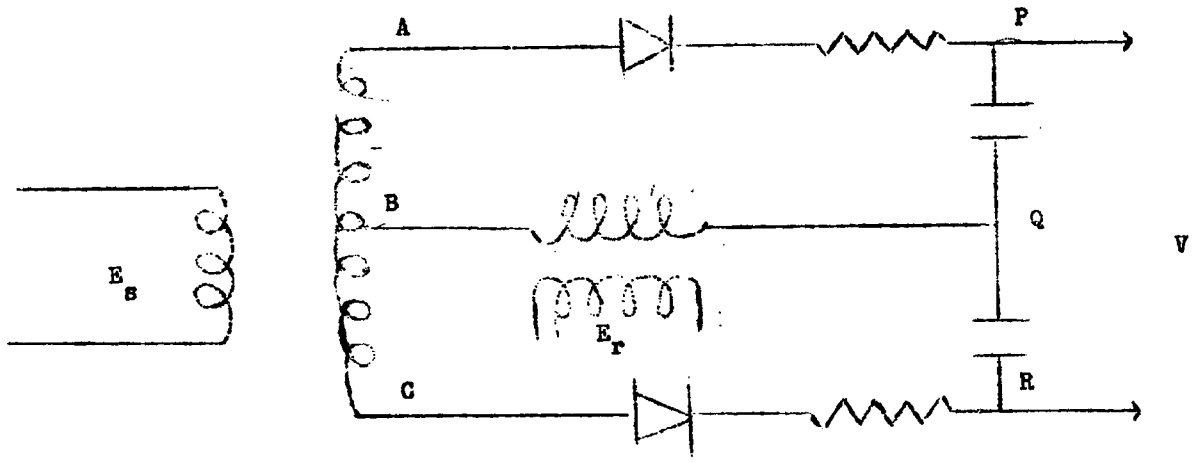

Fig. 4. Phase Detector

Then they can be represented by the functions $E_r \cos\omega t$ and $E_s \cos[\omega t + \Delta t + \phi]$, respectively. Thus the signal input can be interpreted as a signal of the same frequency as the reference, but with a varying phase angle. If $\Delta / \omega \ll 1$, the variation will be slow, and the effective phase shift willlresult in a non-zero value of V. If the system is connected so that a positive value of Δ produces a positive V, this addition to the negative reflector supply will tend to lower the frequency. Thus, if Δ is made small enough, the system will phase-lock with the reference standard.

The klystron can actually lock in on any frequency f_k which will produce a 60 Mc/sec beat with a harmonic of 45 Mc/sec. Hence,

$$| f_k - 45n | = 60 \quad \text{or} \quad f_k = 45\, n \pm 60. \qquad [1]$$

The solutions to Eq. [1] in the vicinity of 3000 Mc/sec are 2940, 2955, 2985, 3000, 3030, and 3045. In addition, frequencies of 2970 and 3015 Mc/sec will be produced as the 66th. and 67th. harmonics of 45 Mc/secs. As the wavemeter in this region has graduations of 1 Mc/sec, there can be no confusion about which one of these frequencies is being utilized. Lock-in at the proper frequency is then a simple matter. First, the phase detector is bypassed [see the switch in Fig. 3.]. The klystron is then tuned to 3000 Mc/sec on the wave meter. A meter on the phase detector will indicate whether or not the frequency is within the proper region. If it is not, small adjustments of the reflector voltage should bring it into range and the by-pass switch can be turned off.

It should be pointed out that using the above stabilization scheme, the absolute uncertainty in the standard frequency is approximately 3000 times that in the 1 Mc/sec oscillator, or 200 times that of WWV.

Figure 5. is a block kiagram of the search frequency stabilizer. The klystron output is attenuated and portions are coupled off to a

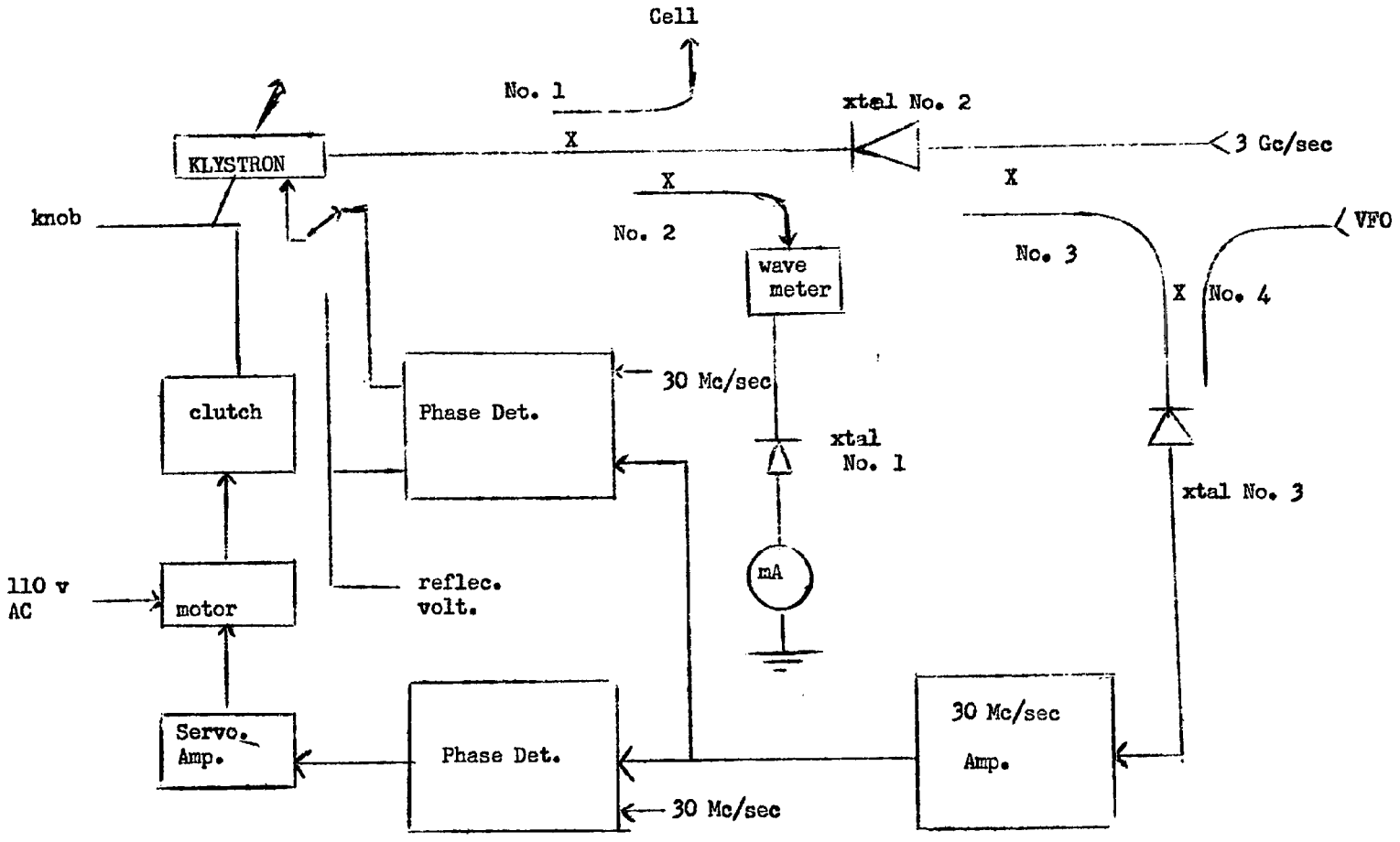

Fig. 5. Search Klystron Stabilization Scheme

wavemeter for frequency measurement and to the cell. The remaining signal enters crystal mount 2., where it is mixed with harmonics of the 3000 Mc/sec standard which is introduced through the side arm of directional coupler 3. The resulting beat frequency, which lies between 0 and 3000 Mc/sec, enters directional coupler 4. and is mixed in crystal mount 3. with harmonics of the VFO frequency [200-500 Mc/sec]. Any 30 Mc/sec beat frequency which is produced in crystal mount 3. enters the IF amplifier and, after phase detection, is used to correct the reflector voltage as before.

The above scheme results in phase-locking of the search klystron to a combination of the 3000 Mc/sec standard and the VFO. By adjusting the frequency of the VFO, f_v, the klystron frequency can be changed; but if the klystron is to follow over any appreciable range, the cavity must be readjusted. This is the reason for phase detector 2. The input signals are the same as for the relfector phase detector, but the time constant is much longer, smoothing out the quick corrections that were necessary there. The amplified output from this unit drives a servo motor which readjusts the cavity to keep the average relector correction zero. In this manner, sweeps can be made as long as the harmonic do not interfere.

Two questions arise concerning the search klystron frequency, namely, how is it determined and what is its uncertainty? When the 1 Mc/sec crystal is used as the frequency standard the uncertainty of the 3000 Mc/sec signal is 3000s, where s is the uncertainty in the 1 Mc/sec standard. The frequency of the search klystron, f_s, is given by

$$\left| f_s - m f_k \pm \ell f_v \right| = 30 \text{ Mc/sec}$$

or

$$f_s = m f_k \pm \ell f_v \pm 30, \qquad [2]$$

where m and ℓ are positive integers. Thus, if the uncertainty in the VFO frequency is s', the overall uncertainty is $\left([3000\ Ms]^2 + [\ell s']^2\right)^{\frac{1}{2}}$. It is easily seen that the VFO frequency can be more than a thousand times more than the standard before it has much effect on the result.

The actual value of f_s is found using Eq. [2] and two pieces of recorded information: the wavemeter value of f_s and the frequency of the VFO as read by a frequency counter. In most cases this will be sufficient to determine the frequency unambiguously, but in a few cases it will not. By way of example, suppose that the wavemeter reads 34,545 ± 2 Mc/sec and f_v is 356.693 804 Mc/sec at the instant of measurement. First, the following approximation is made.

$$34{,}545 = 3000\ m + 357\ \ell \pm 30. \qquad [3]$$

As the strength of the ℓ^{th} harmonic is proportional to $1/\ell$, low numbers are more likely for the constants m and ℓ. By inspection, m values of 11 and 12 correspond to the lowest values of ℓ. Table I shows the possible value of ℓ for some given values of m in Eq. [3]. Any other value of m leads to ℓ greater than 20.

Table I.

m	Eq. [3]	+ ℓ	- ℓ
10	$357\ \ell = 4545 - [\pm 30]$	12.65	12.82
11	$357\ \ell = 1545 - [\pm 30]$	4.24	4.41
12	$357\ \ell = -1455 - [\pm 30]$	-4.16	-3.99
13	$357\ \ell = -4455 - [\pm 30]$	-12.56	-12.68

Table I shows that there is only one combination that is consistent with the data, namely m, ℓ equal to 12, -4, respectively; and the minus sign is used with the 30 Mc/sec. Putting these numbers into Eq. [2] one

obtains

$$f_s = 12\text{x}30.000\ 000 - 4\text{x}356.693\ 804 - 30.000\ 000$$

$$34{,}543.224\ 784 \text{ Mc/sec.}$$

The uncertainty in the above frequency is given by $\left[(36{,}000\ s)^2 + (4\ s')^2\right]^{\frac{1}{2}}$. The quantity s is in this case at least as small as 0.05 cycles/sec (5 parts in 10^8). The VFO frequency has the same instantaneous accuracy as the counter, five parts in 10^8, but variations due to short-term instability will increase the value of s'. Taking $s' = 357$ (1 part in 10^6) the overall uncertainty becomes 1936 cycles/sec. Thus the measured frequency can be written $f_s = 34{,}543.224\ 8 \pm 0.002$ Mc/sec.

The above interpretation of the frequency data can be verified by considering the closest possible alternative. This is the case for m, ℓ equal to 12, -4; and using the plus sign. This frequency calculates to 34,603.224 784 Mc/sec, which is inconsistent with the wavemeter reading.

The lock-in procedure for the search klystron is similar to that for the reference klystron. First the unstabilized klystron is tuned approximately to the desired frequency. A suitable value of f_v is varied slightly, if necessary, to bring the stabilizer within range. For example, suppose lines are observed at about 28,970 Mc/sec. The klystron is tuned to about 28,980 Mc/sec. If m is taken to be 9, ℓf_v is 1980 - 30 Mc/sec, making $f_v = 487.5$ Mv/sec. Upon making this setting, lock-in should be automatic. By sweeping in the direction of decreasing f_v, the region of interest will be searched.

The several detection systems which are now being developed will be described briefly. Figue 6. illustrates three methods by which detection can be accomplished. The first method (a) is the standard

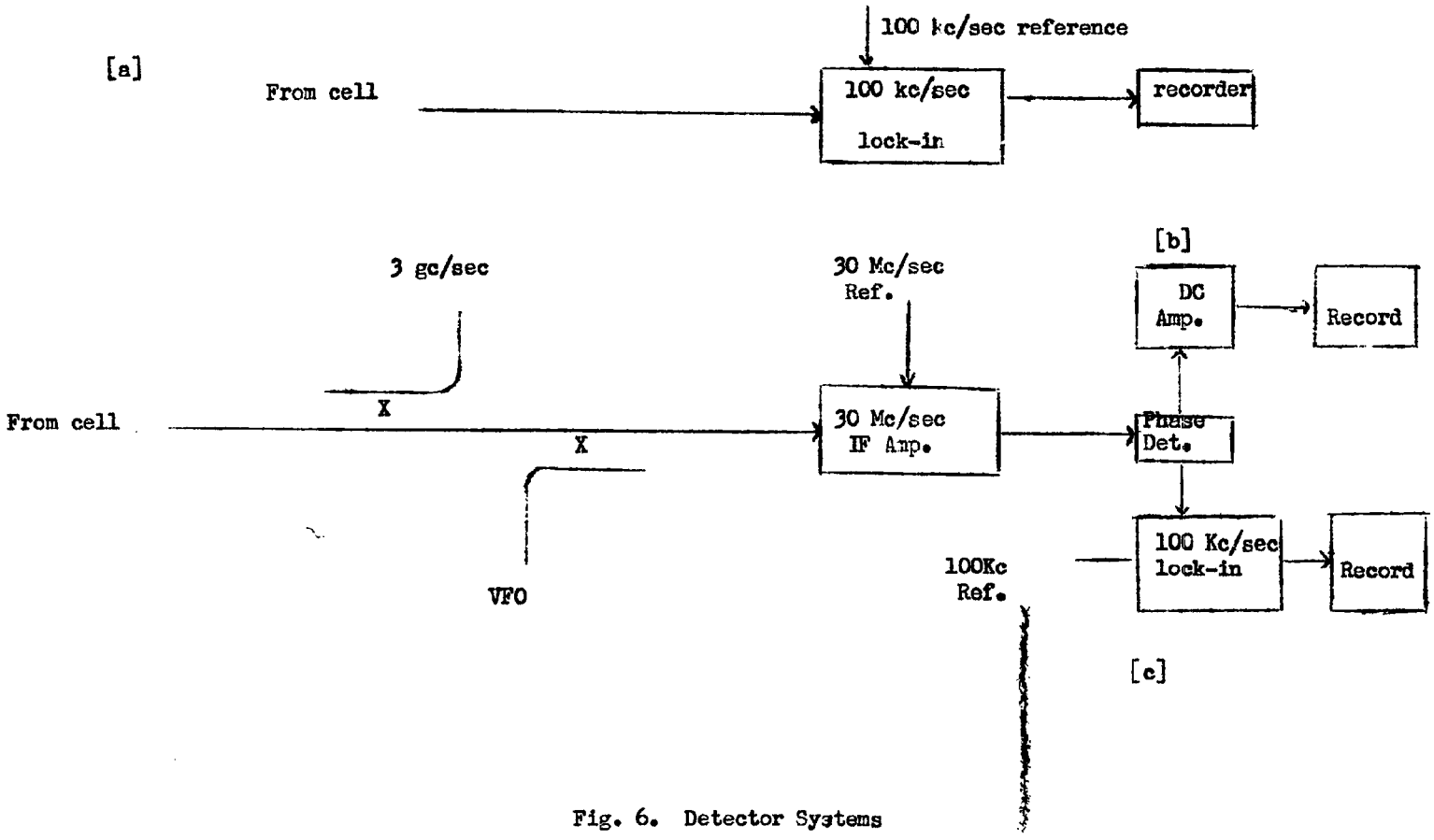

Fig. 6. Detector Systems

one for use with Stark modulation systems. The detected signal is fed into a tuned 100 kc/sec amplifier (the frequency of the Stark modulation); the amplified signal is phase-detected and recorded. The second possibility (b) is to take advantage of the fact that by virtue of the stabilization scheme the correct frequencies are on hand to produce a 30 Mc/sec beat frequency. Lines then appear as an amplitude modulation of the beat. Phase detection of the signal and subsequent DC amplification enable lines to be measured when no modulation is applied. The third method is heterodyned down to 30 Mc/sec and then phase-detected against the 30 Mc/sec standard. The resulting signal is in turn phase-detected against the 100 kc/sec Stark modulator.

The third detection method outlined above would be expected to be the most sensitive. However, in line-shape studies the use of Stark modulation may be objectionable, therefore the second method would be useful. On the otherhand, for relatively strong lines, the flexibility of the first method offers many advantages.

Status of the Project

During the past few months the basic instrument, omitting the frequency stabilization system, has been completed. The Stark modulator was tested and was found to perform well after some minor repairs. Arcing was produced at around 100 volts when the modulator was connected to the Stark cell. The difficulty, which was traced to faulty insulation near the ends of the septum, was rectified. An initial attempt to find one of the J=1 → J=2 transition in OCS failed due to leaks in the cell which prevented the maintainence of a suitable gas pressure. The cell was subsequently completely dismantled and cleaned. All joints were resoldered, the flanges were faced off and the septum was tapered on the ends. The last modification should afford a better match to the rf circuitry and reduce the tendency to arc. A general description of the Stark cell was presented in the Fifth Quarterly Report. The cell now appears to be sufficiently tight so that another attempt to test the instrument on a well-known spectrum can be made immediately.

During the above difficulties work continued on the frequency stabilization system. The complete microwave portion of Fig. 5. was constructed and tested. The frequency standard shown in Fig. 2. was completed. The multiplier section was developed by modifying a Micro-Now Model 101 Frequency Standard.

A Micro-Now Model 201 Frequency Stabilizer was purchased to serve as IF amplifier and detector for the 3 Mc/sec klystron (Fig. 3.). The cavity phase detector for the search klystron was constructed from a circuit developed by Professor Gwinn's group at Berkeley.

Its principle of operation is discussed above in connection with Fig. 4. The unit develops ample voltage to operate the Brown Amplifier-Servo Motor combination.

An improved version of Gwinn's repeller phase detector has been built in breadboard form. This circuit will be used to drive the search klystron.

A 15 Mc/sec IF amplifier was obtained for reception of WWV. The addition of crystal filters should provide sufficiently sharp response characteristics so that the side bands will be eliminated. The resulting clean carrier will then serve as the standard frequency for the system. Alternatively, in the event of poor reception, the 1 Mc/sec time base from the Hewlett-Packard counter can be used with some loss in frequency stability.

At the present time the instrument is complete in the sense that all component units have been obtained or built. However, a considerable amount of work remains to be done in assembling the units and testing the completed instrument.

References

[1] S. Roberts and A. Von Hippel, J. Appl. Phys. 17, 610 [1946].

[2] R. C. LeCraw and E. G. Spencer, IRE Natl. Conv. Record 5, 66 [1956].

[3] E. F. Labuda and R.C. LeCraw, Rev. Sci. Instruments 32, 391 [1961].

[4] C. G. Montgomery, Ed., Technique of Microwave Measurements, McGraw-Hill Book Company, Inc., New York, 1947.

[5] E. D. Reed, Proc. Natl. Electronics Conf. 7, 162 [1951].

[6] Evans, Yoffe and Gray, Chem. Revs. 59, 515 [1959].

APPENDIX. INFRARED SPECTRUM OF SOLID METHYL AZIDE

by

T. E. Whyte, Jr.

This appendix is based on a thesis by Thaddeus E. Whyte, Jr., which was presented in partial fulfillment of the requirements for the M.S. degree at Howard University, 15 May 1962. Earlier work on the infrared spectrum of methyl azide was reported in the First Quarterly Report, Contract DA-44-009-ENG-4763, 27 March to 26 June 1961. The infrared spectrum of methyl azide is now believed to be sufficiently well understood so that no further work on it is planned in this laboratory. However, when the microwave spectrograph is completed, this molecule will be studied in an effort to determine its detailed geometry and the effect of its internal rotation.

A paper based on the present report was presented at the Annual Symposium on Molecular Structure and Spectroscopy, The Ohio State University, June 1962 and is now being prepared for publication in a technical journal.

GCT

INTRODUCTION

Until fairly recently the vibrational spectra of methyl azide had received little attention. An infrared spectrum of methyl azide was first published by Eyster and Gillette[1] in 1939. The absorption spectrum of this compound was studied between 2 and 20 μ at a pressure of 6 cm, using a NaCl prism spectrometer. Pierson, Fletcher and Gantz[2], included a spectrum of methyl azide in a collection of spectra of gaseous molecules. The Raman spectrum of liquid methyl azide was studied by Blum and Verleger[3]. Kohlrausch, et al[4], using the above Raman data, interpreted the spectrum in terms of the electron diffraction work of Pauling and Brookway[5].

In 1961, Fateley and Miller[6] studied methyl azide in the far infrared region. They assigned a band at 126 cm^{-1} to the torsional frequency of the hindered methyl group. In the same year Milligan[7] reported a study of the photolysis of methyl azide in argon and carbon dioxide matrices.

The earlier work of Eyster and Gillette was recently re-examined by Mantica and Zerbi[8]. Methyl azide was studied in the gas phase and in carbon tetrachloride and carbon disulfide solutions, using a Perkin-Elmer Model 21, equipped with sodium chloride, calcium flouride and potassium bromide prisms. For higher resolution a double pass Perkin Elmer Model 112 with calcium flouride and lithium flouride prisms was used. Mantica and Zerbi found that several strong bands in the spectrum reported Eyster and Gillette were due to impurities in the sample, mainly methyl ether.

A study of the spectrum of gaseous, deuterated methyl azide has

recently been completed by Miller and Bassi[9]. In general the work on the deuterated compound supports that of Mantica and Zerbi. However, Miller and Bassis recommend several changes in assignments based primarily on their product rule calculations.

Although the infrared spectrum of methyl azide has been studied in the gas phase, in liquid solution and in inert matrices, no work has been published on the spectrum of the pure solid. A study of the solid might be expected to clear up the conflicts in the assignments by the two most recent authors.

In 1955, Dows and Pimentel[10] reported the spectra of solid and liquid hydrazoic acid. In this work a definite shift was noticed in the C-H stretching and deformation modes of the molecule in passing from the liquid to the solid. The effect was attributed to increased hydrogen bonding in solid hydrazoic acid. A similar shift in these regions should be observed in the spectra of methyl azide if appreciable hydrogen bonding occurs in the solid. Also, changes in the relative intensities of the bonds involving the in-plane and out-of-plane motions should give some insight into any orientation tendencies in the crystalline solid.

From the electron diffraction data of Pauling and Brockway,[5] the structure of the methyl azide molecule is

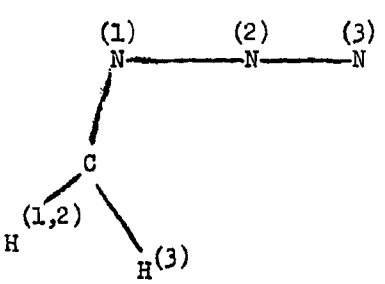

corresponding to the point group C_s. The dimensions fo the molecule are:

$C-N^{(1)}$	1.47±0.02Å
$N^{(1)}-N^{(2)}$	1.24±0.02
$N^{(2)}-N^{(3)}$	1.10±0.02
C-H	1.06 Å
∠ H-C-H	109° 28'
∠ C-N-N-	120± 5°

The 3N - 6 = 15 normal vibrations form the representation $\Gamma = 10a' + 5a''$, with all fundamental frequencies expected to be active in both the Raman and infrared spectra.

EXPERIMENTAL

Two instruments were used to obtain the initial spectra of gaseous and solid methyl azide. The region from 5000 cm^{-1} to 600 cm^{-1} was investigated using a Perkin Elmer Model 21 infrared spectrometer equipped with a sodium chloride prism. The spectra in the region between 4000 cm^{-1} to 2000 cm^{-1} were obtained, using a modified Perkin-Elmer Model 12 spectrometer, which was converted to couble pass and equipped with a lithium flouride prism. The region from 700 cm^{-1} to 400 cm^{-1} was investigated using the modified Model 12 equipped with a KBr prism.

The source optical system of the Model 12 was rebuilt to accomodate a zirconium-arc source and to provide space for the low-temperature cell used in obtaining spectra of solid samples.

The zirconium arc has been constructed from a Sylvania 300 watt concentrated "Western Union" arc [type 300 A.C.]. The lamp is incorporated in the optical system shown in Fig. 1, which is similar to that designed by Wilmot and Brookshier[11]. The light from the arc is focused at F by the spherical mirror M_2. Radiation from F is gathered by the second spherical mirror M_3 and is directed by plane mirror M_4 toward the entrance slit of the monochromator. Due to off-axis aberration, the image of the source is slightly distorted at F. This aberration, however, is partially cancelled at the entrance slit. The globar source G, can be introduced simply by inserting the plane mirror M_4. The spectra of small samples can be obtained much more efficiently than is possible with commercial spectrometers due to the presence of a focal point at F. Because of the small image size of the zirconium arc only a small loss of energy is suffered when the beam is masked at

F to an area of even a few square millimeters.

The entire optical system, including the monochromator, is flushed with laboratory compressed air. Before the air is allowed to pass into the spectrometer, it is conducted through two, three-foot columns. One of these columns contains soda lime and the other activated alumina [alcoa F-1, No. 3-14 mesh soaked in NaOH solution]. The connections from the two columns to the optical apparatus and monochromator were made using copper tubing. An equalizing valve was introduced to maintain an even flow in the source optical system and the monochromator.

The alumnia column is wrapped with nichrome wire insulated with asbestos sheets. The length of the wire was adjusted, so that a temperature of 400° C could be obtained. Attainment of this temperature insures regeneration of the alumina. The alumnia is regenerated by opening the compressed air balbe, and by closing the valve which leads to the soda lime column. This allows the air to by-pass the soda lime and enter the alumina column through copper tubing. The A.C. current is turned on and the nichrome wire heats the alumina column. In this way the alumina can be renewed before each spectrum is observed. With this equipment we were able to eliminate the absorption due to water and carbon dioxide almost completely.

The lithium flouride and potassium bromide prisms used with Model 12 were calibrated using the gases listed in Table I.

TABLE I

Prism	Region [cm^{-1}]	Gas
LiF	3950-3447	H_2O atmospheric
LiF	3200-3100	CH_4*
LiF	3100-2650	HCl*
LiF	2650-2300	HBr*
LiF	2220-2000	CO*
KBr	700-4--	H_2O atmospheric
KBr	700-4--	CH_2OH vapor

*Gases secured from Matheson Co.

A standard, 10 cm gas cell was used in obtaining the calibration spectra. The gas pressure were adjusted to give a convenient absorption for each spectrum. The spectra were then analyzed, using the data from Tables of Wave Numbers for the Calibration of Infra-Red Spectrometers[12].

In comparison with the lithium flouride prism, the postassium bromide prism was rather difficult to calibrate. We had success using atmospheric water and methanol vapor as the calibrating gases. The cover on the source optical system was removed and an atmospheric water vapor spectrum was obtained. Immediately afterwards, a dish of methanol was placed in the source optical system and the plexiglass top replaced. The air inside the source optical system was allowed to become saturated with the methanol vapors for about one hour. After this time, the combined water and methanol vapor spectrum was obtained. This spectrum was then compared with that of Downie, Magoon, Purcell

and Crawford[13].

The frequencies obtained from the spectra in the lithium flouride region were plotted against the drum numbers of the spectrometer. A smooth curve was obtained. The same procedure was followed with the potassium bromide data. To test the potassium bromide calibration, we scanned the region again with the plexiglass top of the source optical system removed. The water bands again coincided with the previous spectrum. In addition, the strong carbon dioxide band was observed at 667 cm^{-1} on our calibration curve. The globar source was used in clibrating both prisms.

The sample of methyl azide was obtained from Professor Darwent of the Department of Chemistry, The Catholic University of America. The sample was prepared according to the procedure of Demroth and Wislicenus[14].

This method has been modified and employed with success by other workers, the most recent procedure being that of Franklin[15]. Sodium azide was methylated with metnyl sulfate. Freshly vacuum-distilled technical grade $[CH_3]_2SO_4$ for Distillation Products was added drop-wise to a basic aqueous solution of sodium azide [purified gade NaN_3] was then removed as a gas. After passing through a calcium chloride drying tube, it was collected at -80° C. The condensate was allowed to warm up and distill through a Bigreaux column. The fraction distilling at 20-21°C was collected. This fraction was then purified further by trap-to-trap distillation in vacuo. The middle fraction distilling from a trap maintained at -80° C to one kept at -196° C was finally collected and stored in a flask.

The mass spectrometer and gas chromatographic analysis showed

a typical sample to be at least 99.6% pure. The sample was stored in a refrigerator as a liquid at a temperature of 0° C.

A glass sampling system was constructed to obtain the spectrum of gaseous methyl azide in the LiF and KBr regions. A glass vessel fitted with stopcock and containing the sample, was attached to the gas handling system by way of a ground glass joint. A closed manometer containing dibutyl phthalate [reagent grade, boiling point 203°-206° C/20 mm] was attached to the same system. The gas coil, which was connected to the system by a ball joint with a two way stopcock, completed the gas sampling system. The system was evacuated for one hour. After closing the stopcock to the gas cell, the sample vessel, which was immersed in liquid nitrogen, was attached to the system.

The vapor pressure of methyl azide at liquid nitrogen temperature is negligible. Thus, we could evacuate the gas sampling system after attaching the sample vessel. After evacuation the second time, the system was closed to the pump. The Dewar flask containing the liquid nitrogen was removed and the methyl azide was allowed to vaporized through the system into the gas cell. When the desired pressure was obtained with the manometer, the gas cell was closed. The liquid nitrogen was replaced to prevent the loss of sample. The spectrum of gaseous methyl azide was then obtained.

Due to the higher intensity of the zirconium arc in the region between 3000 and 2000 cm^{-1} it was used in this region in place of the globar source. To observe the weak overtone and combination bands that appear in the gas spectrum, spectra were observed at increasingly high sample pressures. The pressures ran from approxi-

mately 3 mm to 300 mm of Hg.

In obtaining the spectrum of solid methyl azide in the regions 4000 cm^{-1} to 2000 cm^{-1} and 700 cm^{-1} to 400 cm^{-1}, a similar sampling system was used. In place of the gas cell, a low-temperature cell of the Wagner-Hornig[16] type was used. The manometer was detached and replaced by a simple ball-joint glass plug. The cold cell was slightly modified to contain a thermocouple for monitoring the sample temperature. Iron and constantan thermocouple wires were connected to the brass block of the cold cell which holds the window upon which the methyl azide is sublimed. The leads from the brass block were soldered to small copper wires. The copper-thermocouple joint was then attached to a metal-to-glass seal which was connected to the cold cell by means of iron and constantan wires to a Varian G-11 recorder. The low temperature cell was tested to insure that it was vacuum tight. The recorder was adjusted to indicate the temperature of ice water on one side of the scale and liquid nitrogen on the other. To obtain the desired settings a 12AX7 tube type was used in the recorder, giving a span of 9-20 mv. By substituting a 12AT7 or 12AU7 in the recorder input circuit, a span of 21-50 mv or 51-100 mv, respectively, could be obtained. After the above substitution, the span and gain controls were readjusted to give the desired deflections.

With the low temperature cell in place, the system was flushed for fifteen minutes, and then evacuated. Liquid nitrogen was added to the low-temperature cell until the recorder indicated that the brass block containing the window had reached -180°C. When liquid nitrogen temperature was obtained, the methyl azide sample was allowed

to distill over to the window. As soon as a light haze was formed on the window the stopcock of the cold cell was closed and the methyl azide sample was frozen in the glass storage vessel. After waiting for the window in the brass block to attain approximately -180°C again, the spectrum was recorded.

Several spectra with different sample thicknesses were obtained. Overtones and weak bands were observed using thicker sample films. In the region from 4000 cm^{-1} to 600 cm^{-1} the gas cell and low-temperature cell contained sodium chloride windows. The window in the brass block of the low-temperature cell also contained a sodium chloride window. In the region from 700 cm^{-1} to 400 cm^{-1} potassium bromide windows were used throughout.

It was noted that the efficiency of the flushing system decreased tremendously after one hour. In fact after two hours, due to the saturation of the alumina, the column had to be regenerated. Therefore, as an added precaution in the potassium bromide region, a separate blank was obtained on every spectrum, after each run.

Some time later questions arose regarding the assignments in the hydrogen stretching region. In an attempt to resolve the rotational band contours in the gas-phase spectrum, we reran this spectrum on a Beckman IR-7 spectrometer. This work was made possible by the kind help of Dr. A. G. Maki at N.B.S.

INTERPRETATION OF DATA

In general, the spectrum of solid methyl azide supports both the work of Mantica and Zerbi[8] and Miller and Bassi[9]. However, several changes in interpretation are indicated. The assignments for the gaseous and solid methyl azide are listed in Table II.

In the spectrum of the gas, the hydrogen stretching region is dominated by several overlapping bands. Because of their complex rotational structure, the location of the band centers is very difficult. Mantica and Zerbi assigned the hydrogen stretching fundamentals $\nu_1[a']$, $\nu_2[a']$ and $\nu_{11}[a]$ to the three absorption maxima at 3013 cm^{-1}, 2968 cm^{-1} and 3023 cm^{-1}, respectively. Our LiF prism spectrum of gaseous methyl azide in this region agrees with that of Mantica and Zerbi, although slightly better resolution was obtained in our case due to the higher intensity of the zirconium arc.

In order to locate the band origins with certainty the spectrum of the gas was later rerun on the grating instrument. Features were observed at 2888, 2938, 2966 and 3029 cm^{-1} which could be considered in assigning hydrogen-stretching fundamentals. As there are but three such fundamentals, one of the above features must arise from an overtone or combination, or be due to an impurity. However, none of the frequencies could be explained as overtones or combinations. Furthermore, from photolysis experments Mulligan[7] concluded that the strong band which he observed at 2888 cm^{-1} was undoubtedly due to an impurity. The remaining three bands are assigned to the hydrogen-stretching fundamentals, the particular choice of assignment being dictated by consideration of band shapes and Raman polarization data[4].

If one assumes that the 2888 cm^{-1} feature in the spectrum of the solid is also due to an impurity, the remaining three bands fall fairly close to the hydrogen-stretching fundamentals which were assigned above. One would therefore conclude that there is little or no hydrogen bonding in solid methyl azide. The question of hydrogen bonding in the solid could be considered in more detail if the crystal structure were known. Probably, due to the instability of methyl azide, no x-ray work appears to have been published.

The region from 1250 cm^{-1} to 1500 cm^{-1} in the spectrum of the gas is especially difficult to interpret because of the presence of a number of overlapping bands. The band at 1270 cm^{-1} is without doubt the pseudo-symmetric stretching fundamental ν_6. The structure which exhibits four absorptions maxima in the region 1400 to 1500 cm^{-1} was interpreted by Mantica and Zerbi as a pair of parallel-type bands at 1417 and 1452 cm^{-1}, each consisting of well separated P and R branches. The bands were assigned by those authors to ν_4 and ν_{12}, respectively. The remaining strong band in this region was found at 1330 cm^{-1} [1334 in our work] and was assigned by Mantica and Zerbi to ν_7. Miller and Bassi, however, assign 1452 cm^{-1} [1447 cm^{-1} in their work] to both ν_9 and ν_{12}.

However, the spectrum of the solid [Fig. 3] shows three bands in the region 1400 cm^{-1} to 1500 cm^{-1}. It is therefore probable that the four maxima observed in this region of the gas phase spectrum result from the overlapping of three bands at frequencies of approximately 1417, 1437, and 1460 cm^{-1}. We, therefore, assign these bands to ν_4, ν_5 and ν_{12}, respectively. These assignments allow the strong band at 1334 cm^{-1} to be assigned to $2\nu_9$ in Fermi

TABLE II

ASSIGNMENT OF GASEOUS AND SOLID METHYL AZIDE [Cm^{-1}]

Approx. Descrip.		Gas[a]	Gas[b]	Gas[c]	Solid[c]
CH_3 asym. stretch	ν_1	3018	3023	3029[f]	3035
CH_3 sym. stretch	ν_2	2963	2935	2938[f]	2933
N_3 asym. stretch	ν_3	2186	2106	2106[e] 2100[e]	2208[e] 2177[e] 2114[e]
CH_3 asym. deform.	ν_4	1272	1452	1437	1441
CH_3 sym. deform.	ν_5	910	1417	1417	1410
N_3 "sym" stretch	ν_6	1417	1272	1330[d] 1270[d]	1312[d] 1275[d]
CH_3 in-plane rock	ν_7	1334	1187	1187	1160
CN stretch	ν_8	1035	910	912	909
N_3 in-plane bend	ν_9	555	666	664	667
CNN bend	ν_{10}	259	249	---	---
CH_3 asym. stretch	ν_{11}	3023	2962	2966[f]	2979
CH_3 asym. deform.	ν_{12}	1452	1452	1460	1463
CH_3 out-of-plane wag	ν_{13}	1140	1140	1131	1129
N_3 out-of-plane bend	ν_{14}	666	555	555	559
CH_3 torsional	ν_{15}	---	126	---	---

[a]Data from the work of Mantica and Zerbi.
[b]Data from the work of Miller and Bassi.
[c]Observed in the present work.
[d]One component of Fermi doublet ν_6 and $2\nu_9$.
[e]One component of Fermi triplet ν_3, $\nu_6 + \nu_8$ and $2\nu_9 + \nu_8$.
[f]Data taken with grating instrument.

resonance with ν_6. This Fermi doublet is obviously analogous to the well known [Raman-active] pair ν_1 and 2 ν_2 of CO_2, N_3^-, etc. Its overtone consisting of $2\nu_6$ and $4\nu_9$ which appears at approximately 2525 cm^{-1} in the spectrum of the solid, exhibits the same relative intensity pattern.

It should be pointed out that the above assignments account in detail for the apparent doublet character of the fundamentals ν_6 and ν_3[which are analogous to ν_1 and ν_3 in the spectra of inorganic azides] without recourse to the assumption of a bent azide group[17]. The fact that the spectra of many organic azides show doublets in these two regions[18] would be expected on the basis of the above assignments because all modes involved in the Fermi interactions are roughly confined to the $C^{N---N---N}$ group. The "C----N stretch", ν_8, would be most sensitive to the nature of the remainder of the molecule, since the C---N bond stretching force constant would be expected to vary significantly with electron-drawing power of the rest of the molecule. Because the magnitude of the Fermi interaction is strongly frequency dependent, the relative intensity of the components of the doublet should be quite sensitive to the environment of the $C^{N---N---N}$ group. Hence, in some molecules the interaction may be small, resulting in the observation of only the single stron fundamental.

The bands occurring at 1187 cm^{-1} and 909 cm^{-1} are assigned by Miller and Bassis to ν_7 and ν_9, respectively. The spectrum of solid methyl azide supports these assignments. In the solid, ν_7 occurs at 1160 cm^{-1}, and ν_8 at 909 cm^{-1}.

Mantica and Zerbi have assigned the bands occurring at 259, 666, 555 cm^{-1} to ν_9, ν_{14}, and ν_{10}, respectively. Miller and

Bassi state that the CH_3N_3 Raman polarizations are a useful guide in this region. They suggest that an obious improvement is to change the polarized 656 cm^{-1} frequency in species a' and a". Thus, Miller and Bassi assign 259, 656 and 555 cm^{-1} to ν_9, ν_{14} and ν_{10}, respectively.

In our investigation of the solid, we could not observe the band at 249 cm^{-1} because of the limitations of the instrument. However, the assignments of ν_9 and ν_{14} could be cleared up if one knew the orientation of the methyl azide in the solid. In the region from 700 cm^{-1} to 400 cm^{-1}, we did notice that the relative intensities of the rundamentals absorbing at 553 cm^{-1} and 667 cm^{-1} changed in going from the gas to solid phase. After annealing sample on the KBr window of the low temperqture cell, the bands became stronger and sharper. In the gas phase the fundamental at 667 cm^{-1} was more intense than the band at 559 cm^{-1}. In the solid, however, the intensity was reversed, and the fundamental at 559 cm^{-1} was the stronger.

A similar phenomenon was noted by Mador and Williams[19]. They observed a transition in solid hydrazoic acid occurring at 148°K. The low temperature phase was clear colorless glass and the transition produces a polycrystalline material. Dows and Pimentel[10] observed differences in the phases of solid HN_3. The spectra of the initial solid phase and the second solid phase differed in that the spectrum of the latter was distinctly sharper. The broadness of the bands suggest a certain amount of disorder in the first phase, and this phase may have a glassy structure (as indicated by Mador and Williams), or it may be an unstable disordered crystalline arrangement (due to rapid freezing) which becomes ordered on warming. It is interesting to notice that similar transitions have been reported by Malherbe and Bernstein[20] and Nightingale and Wagner[21]. Our investigation seems to support the above observation that, after the initial coating of the window and subsequent warming, there is ordering or orientation effect. Two possible molecular orientations in the film on the KBr surface of the low temperature cell might be considered. Either the molecule lies so that its plane of symmetry is parallel to the surface of the KBr window or it is sticking out almost perpendicular to the window. If the molecule is oriented with the methyl group sticking our from the plane of the window, then the electric vector of incident radiation is perpendicular to dipole moment derivatives associated with the in-plane motions of the molecule. Thus, one would expect the out-of-plane bending mode to increase in intensity relative to the in-plane mode upon passing from the gas to the solid. However, if the molecule is oriented so that it is lying parallel to the plane of the KBr window, then,

the electric vector is perpendicular to the "N_2" out-of-plane bending mode. Thus, in the latter case one would expect the in-plane bending mode to exhibit increased relative intensity in the solid.

The data from the solid shows that the band arising at 559 cm^{-1} increases in intensity. This spectrum thus seems to support the assignment of Miller and Bassi, in that, the N_2 out-of-plane should be assigned to ν_{14}.

RESULTS

The infrared spectra of solid and gaseous methyl azide have been observed from 4000 cm^{-1} to 400 cm^{-1}. The assignments were discussed and compared with those of Mantica and Zerbi, and Miller and Bassi. A few changes are recommended.

On the basis of the present assignments there is no evidence of hydrogen bonding in the solid. A simple explanation is offered for the doublets which have been observed in the spectra of many organic azides. It is proposed that the doublets arise from Fermi resonances involving vibrational combinations which are relatively insensitive to the environment of the azide group.

Evidence is presented which indicates an orientation tendency in solid methyl azide.

REFERENCES

1 E. H. Eyster and R. N. Gillette, J. Chem. Phys, 8, 369 (1940).

2 R. H. Pierson, A. N. Fletcher and E. St. C. Gantz, Anal. Chem. 28, 1232 (1956).

3 E. Blum and H. Verlager, Physik. Z. 38, 776 (1937).

4 L. Kalovec, K. W. F. Kohlrausch, A. W. Beitz and J. Wagner, Z. Physik, Chem. 1329, 431 (1938).

5 L. Pauling and L. O. Brockway, J. Am. Chem. Soc. 59, 13 (1937).

6 W. G. Fateley and F. A. Miller, Spectrochim. Acta. 17, 357 (1961).

7 D. E. Milligan, J. Chem. Phys. 36, 1491 (1961).

8 E. Mantica and G. Zerbi, Gazz. Chim. Italiana 99, 53 (1960).

9 F. A. Miller and D. Bassi, Spectrochim. Acta 19, 565 (1963).

10 D. A. Dows and G. C. Pimentel, J. Chem. Phys. 23, 1258 (1955).

11 G. B. Wilmot and R. K. Brookshier, NAVORD Report No. 5157, Technical Report No. 88, U. S. Naval Powder Factory, Indian Head, Maryland, 15 June 1956.

12 Tables of Wavenumbers for the Calibration of Infra-Red Spectrometers, International Union of Pure and Applied Chemistry Commission on Molecular Structure and Spectroscopy, Butterworths, Washington, 1961.

13 A. R. Downie, M. C. Magoon, Thomasine Purcell and Bryce Crawford, Jr., J. of the Opt. Soc. of Am. 43 941 (1953).

14 Dimroth and Wislicenus, Ber. 28, 1573 (1905).

15 J. L. Franklin, et al., J. Am. Chem. Soc. 36, 298 (1958).

16 E. L. Wagner and D. F. Hornig, J. Chem. Phys. 18, 296 (1959).

17 J. Dodd and E. Lieber, Proceedings of the Tenth Annual Basic Research Contractors Conference and Symposium, Fort Belvoir, Virginia, 24-26 October 1961.

18 E. Lieber and E. Oftedahl, J. Organic Chem. 24, 1014 (1959).

19 I. L. Mador and M. C. Williams, J. Chem. Phys. 22, 1627 (1954).

[20] F. E. Malherbe and H. J. Bernstein, J. Chem. Phys. 19, 1607 (1951).

[21] R. E. Nightingale and E. L. Wagner, J. Chem. Phys. 22, 203 (1954).